ARTICLE

# Preparation, Characterization and Photocatalytic Activity of Fe, La Co-doped Nanometer Titanium Dioxide Photocatalysts

Zhong-liang Shi, Man Guo, Lin-jun Wang, Shu-hua Yao*

*School of Applied Chemistry, Shenyang University of Chemical Technology, Shenyang 110142, China*

(Dated: Received on April 28, 2015; Accepted on August 1, 2015)

A series of photocatalysts of un-doped, single-doped and co-doped nanometer titanium dioxide ($TiO_2$) have been successfully prepared by template method using $Fe(NO_3)_3{\cdot}9H_2O$, $La(NO_3)_3{\cdot}6H_2O$, and tetrabutyl titanate as precursors and glucan as template. Scanning electron microscopy, X-ray diffraction, and $N_2$ adsorption-desorption measurement were employed to characterize the morphology, crystal structure and surface structure of the samples. The photo-absorbance of the obtained catalysts was measured by UV-Vis absorption spectroscopy, and the photocatalytic activities of the prepared samples under UV and visible light were estimated by measuring the degradation rate of methyl orange in an aqueous solution. The characterizations indicated that the prepared photocatalysts consisted of anatase phase and possessed high surface area of ca. 163−176 $m^2/g$. It was shown that the Fe and La co-doped nano-$TiO_2$ could be activated by visible light and could thus be used as an effective catalyst in photo-oxidation reactions. The synergistic effect of Fe and La co-doping played an important role in improving the photocatalytic activity. In addition, the possibility of cyclic usage of co-doped nano-$TiO_2$ was also confirmed, the photocatalytic activity of codoped nano-$TiO_2$ remained above 89.6% of the fresh sample after being used four times.

**Key words:** Nanometer titanium dioxide, Fe and La co-doping, Photocatalytic activity, Template method, Methyl orange

## I. INTRODUCTION

Photocatalytic oxidation is a potential method for the treatment of organic environmental contaminants, which has received significant interest and research. Among various photocatalysts, titanium dioxide ($TiO_2$) has been extensively used in environmental applications because of its high activity, chemical stability, robustness against photocorrosion, low toxicity, no-twain pollution and availability at low cost so far, especially for the detoxification of water and air [1–4]. However, practical applications of photocatalysis are limited because of two obvious problems arising from fine $TiO_2$ powders, the first broblem is low photoefficiency, and the second problem is separation of fine particles of used $TiO_2$ after the treatment process and the recycling of the photocatalyst [5]. An efficient process that shifted the optical response of active $TiO_2$ from the UV to the visible spectral range and to longer wavelength was doping elements, which could provide a framework to more easily incorporate the photocatalytic and solar efficiency of this material [6–8]. At present, the investigations about doping elements on $TiO_2$ focused mostly on transition metal ions doping [9–11] and rare earth metal doping [12, 13]. It is generally recognized that the substitutional doping of $TiO_2$ with iron Fe(III) has a profound effect on the photoreactivity of $TiO_2$-based photocatalysis through reducing the electron-hole pair recombination rate [14, 15]. Rare earth metals having incompletely occupied 4f and empty 5d orbitals often serve as catalyst or promote catalysis. Some results showed that lanthanum, as one of the rare earth metals, has the ability to enhance the photocatalytic activity of $TiO_2$ [16–19]. Lanthanide doping was proven to increase the surface area, pore volume, adsorption capacity for organic compounds as well as to suppress electron-hole recombination rates during the process of photocatalytic reaction [20, 21]. In recent years, some reports indicated that introducing two or more proper elements into nanocrystalline $TiO_2$ particles would improve the photocatalytic effect of $TiO_2$ [22, 23]. So co-doping transition metal ions and rare earth metal into the nanocrystalline $TiO_2$ may have a synergistic effect on increasing the activity of $TiO_2$.

In order to eliminate the second problem, supported $TiO_2$ is an alteration for the field application of the photocatalyst. Therefore, much recent work has been devoted to immobilizing $TiO_2$ photocatalyst on porous supporting matrices, such as silica [24], alumina [25], zeolites [26], activated carbon [27, 28] and activated carbon fiber [29, 30]. However these methods largely decrease the surface area of $TiO_2$, showing disadvan-

*Author to whom correspondence should be addressed. E-mail: ysh1997@163.com

 

tage: the smaller the surface area, the lower the photocatalytic activity to decompose waste. In the present work, we used $Fe(NO_3)_3{\cdot}9H_2O$, $La(NO_3)_3{\cdot}6H_2O$, and tetrabutyl titanate ($Ti(OC_4H_9)_4$) as precursors and glucan as template to prepare nanometer titanium dioxide photocatalyst co-doped with Fe and La. The photocatalytic activity was evaluated by photodegradation of methyl orange (MO) over the prepared samples under UV and visible light. The synergistic effect of two dopants that led to the significant enhancement of photodegradation was discussed. Additionally, the cyclic performance of co-doped nano-$TiO_2$ for the degradation of MO was also checked.

## II. EXPERIMENTS

### A. Preparation of photocatalysts

In a typical synthesis, 0.01 mol (3.4 g) of $Ti(OC_4H_9)_4$ (analytic grade, Shanghai Xingta Co., Ltd., China) was added to a solution containing 1.0 g of glucan and 8.0 mL of anhydrous ethanol to obtain solution A. A certain amount of $Fe(NO_3)_3{\cdot}9H_2O$ and $La(NO_3)_3{\cdot}6H_2O$ was dissolved in the mixture of 2.0 mL of deionized water, 1.5 mL of glacial acetic acid, and 8.0 mL of anhydrous ethanol at room temperature to gain solution B. The solution A was added drop-wise into the solution B within 60 min by separating funnel while keeping the reaction mixture vigorously magnetically stirred. The resulting white slurry was stirred continuously for 1 h, aged for 48 h at room temperature, and dried for 10 h at 100 °C under reduced pressure to gain the xerogel. The resultant xerogel was crushed to obtain fine powder and further calcined at 500 °C for 2 h to remove the residual organic compounds resulting from the hydrolysis of the $Ti(OC_4H_9)_4$ and the surfactant to prepare the co-doped photocatalyst. The calcined samples were labeled as $Fe_xLa_y$-$TiO_2$, where $x$ and $y$ corresponded to the initial mole ratios of Fe to Ti and La to Ti, respectively.

### B. Characterization

The morphologies of different samples were examined by a scanning electron microscope (SEM, Holland Philips, JSM-5800). Wide-angle X-ray powder diffraction (XRD) patterns of all samples were obtained at room temperature with a Rigaku D/max-r B X-ray diffractometer using Cu K$\alpha$ radiation which was operated at 45 kV and 40 mA. The size of the crystallite was calculated from X-ray line broadening from the Scherrer equation: $D{=}0.89\lambda/\beta\cos\theta$, where $D$ is the average crystal size in nm, $\lambda$ is the Cu K$\alpha$ wavelength (0.15406 nm), $\beta$ is the full-width at half-maximum, and $\theta$ is the diffraction angle. Information about specific surface area and pore volume of catalysts was calculated using the BET method [31] from nitrogen adsorption-desorption isotherms measured at 77 K with a Micromeritics 2000 instrument (ASAP 2000, Micromeritics, USA). UV-Vis adsorption spectroscopy measurements were performed by using a UV-Vis diffuse reflectance spectrophotometer (Shimadzu UV-2550). Reflectance spectra were referenced to $BaSO_4$. The band gap energies ($E_g$) of the prepared photocatalysts was calculated by the formula $E_g{=}1239.8/\lambda_g$ from the wavelength values corresponding to the intersection point of the vertical and horizontal parts of the spectra ($\lambda_g$) [32].

### C. Measurement of photocatalytic efficiency

The photocatalytic activities of the prepared catalysts were studied by degradation experiments using MO (20 mg/L) as model compound in an aqueous solution without concerning the degradation intermediates in detail.

UV light irradiation experiments were carried out using a magnetically stirred quartz reactor and an ultraviolet mercury lamp (150 W, 365 nm) at ambient temperature of about 20 °C. Sixty minute adsorption time in dark condition was allowed before the start of photoreactions. Then samples of the suspension were withdrawn after a definite time interval and filtered through 0.22 μm filter paper. The filtrates were analyzed for residual MO concentration using a UV-Vis spectrophotometer (Shimadzu UV-2550). For comparison, the pure nano-$TiO_2$ and single-doped nano-$TiO_2$ were used as reference systems.

The experiments with visible light irradiation were performed at ambient temperature of about 20 °C by using a 150 W metal halide lamp as the light source. To limit the irradiation wavelength, the light beam was passed through a 410 nm cut filter (L41) to assure cut-off wavelengths shorter than 410 nm. Then, samples of the suspension were withdrawn after a definite time interval and filtered through 0.22 μm filter paper to analyze the residual MO concentration.

## III. RESULTS AND DISCUSSION

### A. Characterization

Figure 1 shows the SEM images of the pure $TiO_2$ and $Fe_{0.005}La_{0.003}$-$TiO_2$. It could be observed that the samples were approximately present in the form of spherical particle and the particles of pure $TiO_2$ congregated together more densely than those of $Fe_{0.005}La_{0.003}$-$TiO_2$. Specific surface area and pore volume of the prepared catalysts are summarized in Table I. As shown in Table I, the measured BET surface areas of all samples had high surface area (163−176 $m^2/g$), and the co-doped samples have higher surface area than pure and single-doped $TiO_2$, the $Fe_{0.005}La_{0.003}$-$TiO_2$ sample

DOI:10.1063/1674-0068/29/cjcp1504084 

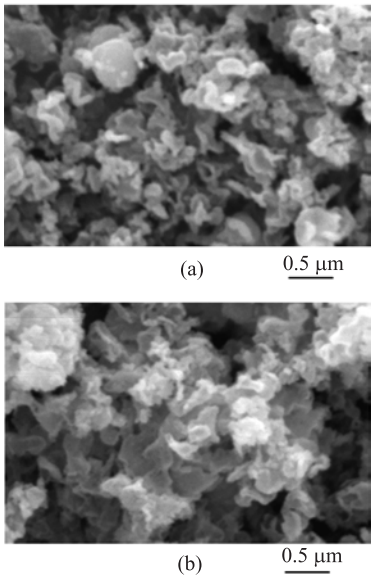


FIG. 1 SEM images of samples. (a) $Fe_{0.005}La_{0.003}$-$TiO_2$, (b) $TiO_2$.

TABLE I The physicochemical properties of pure and doped nano-$TiO_2$. Total pore volume $V_p$ (in $cm^3/g$), average pore diameter $d$ (in nm).

| Sample | $S_{BET}/(m^2/g)$ | $V_p$ | $d$ | $E_g$/eV |
|---|---|---|---|---|
| $TiO_2$ | 164 | 0.337 | 12.2 | 3.22 |
| $Fe_{0.005}$-$TiO_2$ | 163 | 0.339 | 11.3 | 3.17 |
| $La_{0.003}$-$TiO_2$ | 167 | 0.336 | 10.5 | 3.09 |
| $Fe_{0.005}La_{0.003}$-$TiO_2$ | 176 | 0.368 | 10.2 | 2.95 |

displays the highest specific surface area 176 $m^2/g$ and the highest pore volume 0.368 $cm^3/g$.

To obtain information of the crystal structure of the prepared photocatalysts, X-ray diffraction patterns were measured. The XRD patterns of prepared samples are shown in Fig.2. It could be seen that all prepared $TiO_2$ were present in the anatase phases and there was no evident difference among pure $TiO_2$, $Fe_{0.005}$-$TiO_2$, $La_{0.003}$-$TiO_2$, and $Fe_{0.005}La_{0.003}$-$TiO_2$. The diffraction peaks at 25.38°, 37.80°, 48.05°, 55.07°, and 70.25° are consistent with the (101), (004), (200), (105), and (220) peaks of anatase titanium dioxide. The XRD results suggested that Fe and La co-doping has little influence on the nature of crystal formation. The physical properties determined from XRD data of the samples are listed in Table II, it could be seen that the crystallite sizes decrease because of the doping, which implies that Fe and La doping restrains the increase in grain size and refines crystallite size. Compared with pure $TiO_2$ ($a$=$b$=0.3778 nm and $c$=0.9516 nm), it was clear that the lattice parameters $a$ and $b$ of the doped samples remained almost unvaried while the parameters $c$ decreased. This demonstrated that the crystal lattices of the as-prepared samples were locally distorted by doping.

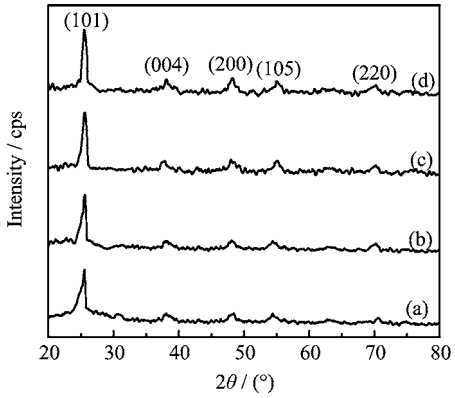


FIG. 2 XRD patterns of samples. (a) $TiO_2$, (b) $Fe_{0.005}$-$TiO_2$, (c) $La_{0.003}$-$TiO_2$, (d) $Fe_{0.005}La_{0.003}$-$TiO_2$.

TABLE II XRD analysis results of samples.

| Sample | $X^a$/nm | Lattice parameters | | |
|---|---|---|---|---|
| | | $a$/nm | $c$/nm | $V/nm^3$ |
| $TiO_2$ | 11.8 | 0.3778 | 0.9516 | 0.1358 |
| $Fe_{0.005}$-$TiO_2$ | 11.2 | 0.3782 | 0.9515 | 0.1361 |
| $La_{0.003}$-$TiO_2$ | 11.5 | 0.3776 | 0.9494 | 0.1354 |
| $Fe_{0.005}La_{0.003}$-$TiO_2$ | 10.9 | 0.3774 | 0.9482 | 0.1351 |

[a] $X$: crystallite size

UV-Vis absorption spectra were recorded to characterize the light absorption ability of the prepared photocatalysts. Figure 3 shows the UV-Vis absorption spectra of pure, Fe-doped, La-doped and co-doped $TiO_2$, respectively. Modification of $TiO_2$ with Fe and La significantly affected the absorption properties of photocatalysts. Compared with $TiO_2$, there was strong photoabsorption in the visible region (420−700 nm) for the co-doped $TiO_2$ photocatalysts. The red shift of the absorption edge implied a decrease in the band gap energy. The $E_g$ of the prepared photocatalysts are listed in Table I. For pure $TiO_2$ prepared without any dopant, $E_g$ is 3.22 eV. In the case of doped $TiO_2$, $E_g$ decreased from 3.17 eV to 2.95 eV. The lowest $E_g$ (2.95 eV) was observed for sample $Fe_{0.005}La_{0.003}$-$TiO_2$. It was clear that doping led to a modification of the electronic structure around the conduction band edge of $TiO_2$, thus resulted in the band gap narrowing.

### B. Photocatalytic activity

Photocatalytic activity of Fe and La co-doped nanometer titanium dioxide samples was estimated by measuring the degradation rate of MO (20 mg/L) with-

DOI:10.1063/1674-0068/29/cjcp1504084 

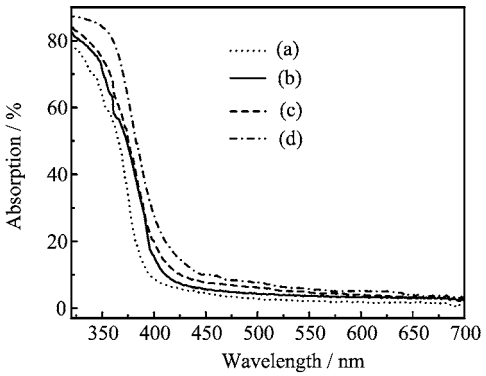


FIG. 3 UV-Vis absorption spectra of samples. (a) $TiO_2$, (b) $Fe_{0.005}$-$TiO_2$, (c) $La_{0.003}$-$TiO_2$, (d) $Fe_{0.005}La_{0.003}$-$TiO_2$.

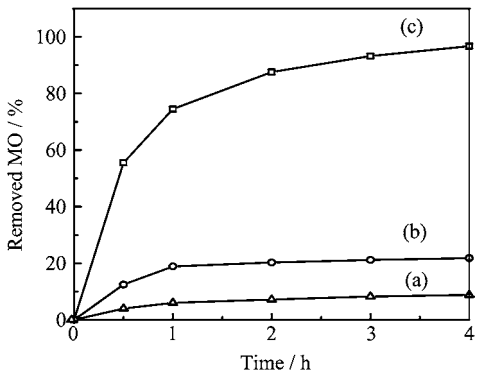


FIG. 4 MO removal processes under different condition. (a) Only with UV irradiation, (b) $Fe_{0.005}La_{0.003}$-$TiO_2$ without UV irradiation, and (c) $Fe_{0.005}La_{0.003}$-$TiO_2$ with UV irradiation.

out concerning the degradation intermediates in detail. Pure and single-doped titanium dioxide synthesized by the same method were used as the reference systems.

In order to evaluate the actual photocatalytic activity of the $Fe_{0.005}La_{0.003}$-$TiO_2$ photocatalyst, three MO removal processes, namely, photolysis of MO, photocatalytic degradation of $Fe_{0.005}La_{0.003}$-$TiO_2$, and adsorption of $Fe_{0.005}La_{0.003}$-$TiO_2$, were compared by assessing the effect of catalyst on the overall removal rate for an initial MO concentration of 20 mg/L, the results were shown in Fig.4. It can be seen from Fig.4 that MO is degraded a little under UV light irradiation without the catalyst (Fig.4(a)). The adsorption of MO on $Fe_{0.005}La_{0.003}$-$TiO_2$ is saturated after 60 min and the removal percentage of MO does not increase any further on prolonging of adsorption time (Fig.4(b)). The degraded percentages of MO increase with increasing UV light irradiation time for MO/$Fe_{0.005}La_{0.003}$-$TiO_2$ system (Fig.4(c)). By comparing the removal percentages of MO with and without UV light (Fig.4), it is affirmed that the disappearance of MO molecules is due to photocatalytic degradation instead of only adsorption.

MO degradation under UV irradiation in the presence of Fe-doped $TiO_2$ with Fe-doped content in the range of 0.2mol%−0.8mol% was investigated (Fig.5). The photocatalytic activity of $TiO_2$ enhanced after Fe-doping with the optimum content of Fe-doping being 0.5mol% (Fig.5). It can be seen from Fig.5 that the degradation percentage of MO using the 0.5mol% Fe-doped $TiO_2$ with UV light irradiation of 4 h reached 92.5%, which is 10% higher than that of pure $TiO_2$. From the UV-Vis absorption spectra of samples (Fig.3), it could be seen that the intensity of UV light photoabsorption on Fe-doped $TiO_2$ was stronger than that of pure $TiO_2$. The strong absorption is beneficial to the photocatalytic activity because the available photons are proportional to photoabsorption. The photoactivity of the catalyst increased gradually with increase in Fe-doping up to 0.5mol%. However, the photoactivity of the catalyst decreased when the content of Fe-doping reached

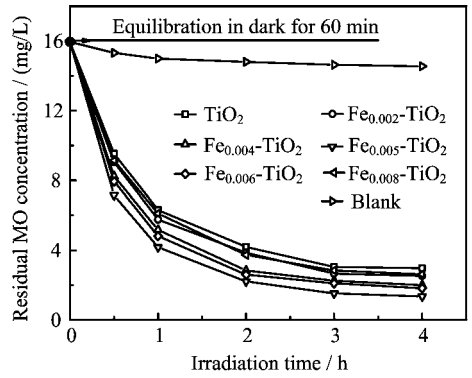


FIG. 5 Effect of Fe-doped content on the degradation of MO under UV irradiation.

0.6mol%. This indicates that with a heavy doping the dopants become recombination centers of the photoexcited electrons, thus reducing the photocatalytic activity. Consequently, it is understandable that there is an optimum Fe-doped content.

Figure 6 shows the results of MO degradation with irradiation time under UV light irradiation in the presence of Fe, La co-doped nanometer $TiO_2$ photocatalysts. It can be seen that all as-prepared samples exhibit higher photocatalytic activity than pure and single-doped $TiO_2$ under UV light. It can be also seen that the co-doped content of the as-prepared samples has an effect on the degradation ratios. Among the co-doped samples, the best performance is attributed to $Fe_{0.005}La_{0.003}$-$TiO_2$ catalyst. It can be calculated that the photocatalytic performance of $Fe_{0.005}La_{0.003}$-$TiO_2$ is almost 1.4 times higher than that of pure $TiO_2$ for degradation of MO under UV light. This may be due to the positive effect of the introduction of Fe and La on the photocatalytic activity since the co-doping not only increases the surface area of $TiO_2$ but also improves its UV absorption. The surface area is one of

DOI:10.1063/1674-0068/29/cjcp1504084 

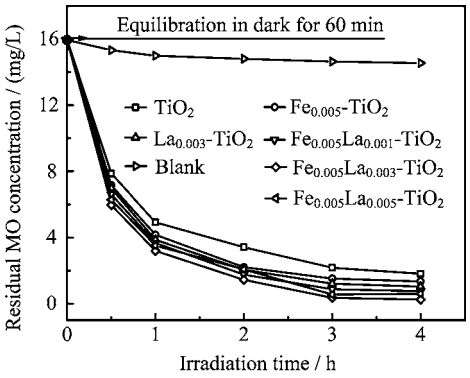


FIG. 6 Degradation curves of MO with different UV light irradiation time in the presence of different photocatalyst.

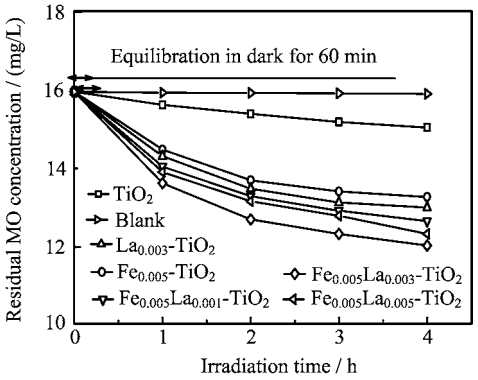


FIG. 7 Degradation curves of MO with different visible light irradiation time in the presence of different photocatalyst.

the key factors to control the photocatalytic activity of a photocatalyst. The larger the surface area is, the higher the photocatalytic activity is. Furthermore, the photoabsorption characters greatly affect the photocatalytic activity of a photocatalyst, since the number of absorbed photons directly depends on the absorption property of the photocatalyst. Obviously, the photocatalytic activity of Fe and La co-doped $TiO_2$ under UV light demonstrates that Fe and La co-doping effect is outstanding. Such an improvement implies that there is a synergistic effect in the photocatalytic activity when both Fe and La are co-doped into the $TiO_2$ catalyst.

Photocatalytic activities of different samples under visible light are shown in Fig.7. It was observed that all samples exhibited photocatalytic activity under visible light. Among the samples, $Fe_{0.005}La_{0.003}$-$TiO_2$ showed the best photocatalytic performance corresponding to the maximum red shift in the UV-Vis absorption spectra (Fig.3). The photocatalytic performance of $Fe_{0.005}La_{0.003}$-$TiO_2$ is almost 4 times higher than that of pure $TiO_2$ for degradation of MO under visible light, which is in agreement with the results of the optical absorption spectra analysis.

### C. Recyclability performances of $Fe_{0.005}La_{0.003}$-$TiO_2$ catalyst

Figure 8 shows the cyclic performance of the $Fe_{0.005}La_{0.003}$-$TiO_2$ photocatalyst without treatment. It was observed that MO could be degraded by the prepared photocatalyst under UV irradiation. The photocatalytic reactivity was only slightly reduced in stirred aqueous solution and the $Fe_{0.005}La_{0.003}$-$TiO_2$. After being used four times, ca. 89.6% of photocatalytic activity of the fresh sample remained (Fig.8). The degradation percentage of MO reached 86.7% when irradiation time was 4 h. Thus it is suggested that the final removal of MO from solutions was caused by the photocatalytic degradation rather than the adsorption process that leads to saturated adsorption of MO on the photo-

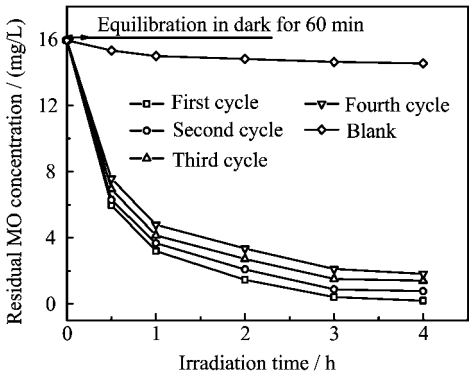


FIG. 8 The recyclability performance of $Fe_{0.005}La_{0.003}$-$TiO_2$ catalyst.

catalyst. These results indicated that the cyclic usage of $Fe_{0.005}La_{0.003}$-$TiO_2$ was possible and its stability in treating polluted water was satisfactory. Therefore, it is potentially employable for continuous photocatalytic degradation processes.

## IV. CONCLUSION

A series of photocatalysts of Fe and La co-doped nanometer titanium dioxide have been successfully prepared by template method using $Fe(NO_3)_3{\cdot}9H_2O$, $La(NO_3)_3{\cdot}6H_2O$ and $Ti(OC_4H_9)_4$ as precursors and glucan as template. The photocatalyst thus prepared was applied to degrade model contaminated water of MO. The results showed that the prepared photocatalyst only contained anatase phase, Fe and La co-doping caused absorption spectra of nanometer titanium dioxide to shift to the visible region and enhanced the photocatalytic activity of titanium dioxide under UV and visible light irradiation. The doping content had an effect on the photocatalytic activity of the photocatalyst, $Fe_{0.005}La_{0.003}$-$TiO_2$ exhibited the optimum photocatalytic activity for MO degradation. The synergistic

DOI:10.1063/1674-0068/29/cjcp1504084 

effect of Fe and La co-doping was responsible for improving the photocatalytic performance.

## V. ACKNOWLEDGMENTS

This work is supported by the National Natural Science Foundation of China (No.41373127) and the program for Liaoning Excellent Talents in University of China (No.LR2015052).

[1] C. Young, T. M. Lim, C. Chiang, J. Scott, and R. Amal, Appl. Catal. B **78**, 1 (2008).
[2] A. C. Rodrigues, M. Boroski, N. S. Shimada, J. C. Garcia, J. Nozaki, and N. Hioka, J. Photochem. Photobiol. A **194**, 1 (2008).
[3] E. I. Seck, J. M. Doña-Rodríguez, C. Fernández-Rodríguez, O. M. González-Díaz, J. Araña, and J. Pérez-Peña, Appl. Catal. B **125**, 28 (2012).
[4] Z. L. Shi, H. Lai, S. H. Yao, and S. F. Wang, Chin. J. Chem. Phys. **25**, 96 (2012).
[5] Y. Zheng, E. Shi, Z. Chen, W. Li, and X. Hu, J. Mater. Chem. **11**, 1547 (2001).
[6] R. Asahi, T. Morikawa, T. Ohwaki, K. Aoki, and Y. Taga, Science **293**, 269 (2001).
[7] C. Burda, Y. Lou, X. Chen, A. C. S. Samia, J. Stout, and J. L Gole, Nano Lett. **3**, 1049 (2003).
[8] I. N. Martyanov, S. Uma, S. Rodrigues, and K. J. Klabunde, Chem. Comm. **21**, 2476 (2004).
[9] J. C. Wu and C. H. Chen, J. Photochem. Photobiol. A **163**, 509 (2004).
[10] C. Wang, C. Böttcher, D. W. Bahnemann, and J. K. Dohrmann, J. Nanoparticle Res. **6**, 119 (2004).
[11] J. Xu, M. Lu, X. Guo, and H. Li, J. Mol. Catal. A **226**, 123 (2005).
[12] K. V. Baiju, C. P. Sibu, K. Rajesh, P. Krishna Pillai, P. Mukundan, K. G. K. Warrier, and W. Wunderlich, Mater. Chem. Phys. **90**, 123 (2005).
[13] A. W. Xu, Y. Gao, and H. Q. Liu, J. Catal. **207**, 151 (2002).
[14] I. Djerdj and A. M. Tonejc, J. Alloys Compd. **413**, 159 (2006).
[15] J. Moser, M. Gratzel, and R. Gallay, Helv. Chim. Acta **70**, 1596 (1987)
[16] I. Atribak, I. S. Bansanez, A. B. Lopez, and A. G. Garcia, Catal. Communn. **8**, 478 (2007).
[17] T. Ando, T. Wakamatsu, K. Masuda, N. Yoshida, K. Suzuki, S. Masutani, I. Katayama, H. Uchida, H. Hirose, and A. Kamimot, Appl. Surf. Sci. **255**, 9688 (2009).
[18] H. H. Wu, L. X. Deng, S. R. Wang, B. L. Zhu, W. P. Huang, S. H. Wu, and S. M. Zhang, J. Disper. Sci. Technol. **31**, 1311 (2010).
[19] K. Dai, T. Peng, H. Chen, J. Liu, and L. Zan, Environ. Sci. Technol. **43**, 1540 (2009).
[20] H. R. Kim, T. G. Lee, and Y. G. Shul, J. Photochem. Photobiol. A **185**, 156 (2007).
[21] F. B. Li, X. Z. Li, and M. F. Hou, Appl. Catal. B **48**, 185 (2004).
[22] J. Wang, S. Yin, M. Komatsu, and T. Sato, J. Eur. Ceram. Soc. **25**, 3207 (2005).
[23] Z. Zhang, C. Wang, R. Zakaria, and J. Y. Ying, J. Phys. Chem. B **102**, 10871 (1998).
[24] L. J. Alemany, M. A. Banares, E. Pardo, F. Martin, M. Galan-Fereres, and J. M. Blasco, Appl. Catal. B **13**, 289 (1997).
[25] W. Q. Huang, A. J. Duan, Z. Zhao, G. F. Wan, G. Y. Jiang, T. Dou, K. H. Chung, and J. Liu, Catal. Today **131**, 314 (2008).
[26] S. Fukahori, H. Ichiura, T. Kitaoka, and H. Tanaka, Environ. Sci. Technol. **37**, 1048 (2003).
[27] J. M. Herrmann, J. Laine, and J. Matos, J. Catal. **200**, 10 (2001).
[28] T. Tsumura, N. Kojitari, H. Umemura, M. Toyoda, and M. Inagaki, Appl. Surf. Sci. **196**, 429 (2002).
[29] S. H. Yao, J. Y. Li, and Z. L. Shi, Particuology **8**, 272 (2010).
[30] S. H. Yao, Y. F. Jia, Z. L. Shi, and S. L. Zhao, Photochem. Photobiol. **86**, 1215 (2010).
[31] S. J. Gregg and K. S. W. Sing, *Adsorption, Surface Area and Porosity*, 2nd Edn., London: Academic Press, (1982).
[32] L. Körösi and I. Dėkány, Colloids Surf. A **280**, 146 (2006).

DOI:10.1063/1674-0068/29/cjcp1504084 